ETH
Eidgenössische Technische Hochschule Zürich
Swiss Federal Institute of Technology Zurich

Seminar for Applied Mathematics SAM

Frequency-Stable Full Maxwell in Electro-Quasistatic Gauge

J. Ostrowski and R. Hiptmair

Research Report No. 2020-43

June 2020
Latest revision: May 2021

Seminar für Angewandte Mathematik
Eidgenössische Technische Hochschule
CH-8092 Zürich
Switzerland

FREQUENCY-STABLE FULL MAXWELL IN ELECTRO-QUASISTATIC GAUGE*

JÖRG OSTROWSKI† AND RALF HIPTMAIR‡

Abstract. The electro-quasistatic approximation of Maxwell's equations is commonly used to model coupled resistive/capacitive phenomena at low frequencies. It neglects induction and becomes unstable in the stationary limit. We introduce a stabilization that prevents this low-frequency breakdown. It results in a system for the electric scalar potential that can be used for electro-quasistatics, electrostatics as well as DC-conduction.

Our main finding is that the electro-quasistatic fields can be corrected for magnetic/inductive phenomena at any frequency in a second step. The combined field from both steps is a solution of the full Maxwell's equations that consistently takes into account all electromagnetic effects. Electro-quasistatics serves as a gauge condition in this semi-decoupled procedure to calculate the electromagnetic potentials. We derive frequency-stable weak variational formulations for both steps that (i) immediately lend themselves to finite-element Galerkin discretization, and (ii) can be equipped with so-called ECE boundary conditions, which facilitate coupling with external circuit models.

Key words. Maxwell's equations, ECE boundary conditions, quasi-static models, low-frequency breakdown, low-frequency stabilization, finite-element method

AMS subject classifications. 35Q61, 65N30, 65N12

1. Introduction.

The full Maxwell equations describe all electromagnetic phenomena at any frequency. So why are they not universally used to calculate electromagnetic fields? Two reasons came to our minds:

The first is that in most situations we observe a near decoupling of capacitive and inductive effects at very low frequencies, and either capacitive or inductive effects dominate, see also [6, 13]. Especially for capacitive settings it is then more efficient to just solve for the electric scalar potential, neglect induction and omit the costly calculation of the magnetic field. Similarly, efficient approximate models for inductive settings that neglect capacitive effects are also well established, the eddy current models [1]. However, these approximate models cannot be applied in situations in which both inductive and capacitive effects matter. As a consequence users of simulation software are forced to select the appropriate model a priori for the specific phenomenon that they want to simulate. Directly solving the full Maxwell's equations would render unnecessary this often problematic choice.

Another reason for eschewing full Maxwell numerical models is their notorious low-frequency instability. Robust formulations that avoid this instability have been developed in recent years, see [2, 5, 7, 9, 11, 12, 14–16]. A good overview of the approaches is given in [5], where the authors devise a symmetric electric field based formulation that uses a minimal number of unknowns for problems with source currents. In [7] the authors introduced a formulation for more general scenarios, also allowing excitation through boundary conditions. This work relies on that approach for stabilization in the low frequency limit. It boils down to explicitly including Gauss's law in the non-conducting domain. Yet, hitherto all the proposed stabilization techniques couple capacitive and inductive effects and needlessly incur high computational cost in electro(-quasi)static settings.

In this article we will show that *full Maxwell computations are a viable option*

*Submitted to SIAM J. Scientific Computing, July 2020.

†ABB Switzerland Ltd, Corporate Research (joerg.ostrowski@ch.abb.com).

‡ETH Zürich, Seminar for Applied Mathematics (ralf.hiptmair@sam.math.ethz.ch).

even at low frequencies and when coupling with circuits has to be taken into account. We introduce a gauge that cleanly decouples

(i) the calculation of the electric scalar potential, accounting for capacitive effects, in a first step from
(ii) the calculation of the magnetic vector potential, accounting for inductive effects, in a second step.

This *two-step approach* to the full Maxwell equations can be deployed at any frequency and nicely reflects the decoupling of capacitive and inductive effects at very low frequencies. It is no longer necessary to rely on an approximate model because both steps can be executed efficiently. In purely electro(-quasi)static settings it is even possible to solve for the electric scalar potential only, and to skip the second step.

The plan of the paper is as follows: In section 2 we will first introduce the (six) customary electromagnetic model equations in frequency domain and potential formulations. Our focus is on low-frequency models. Then we will outline the gist of our approach in section 3. It represents a unification of all electromagnetic models that were presented in section 2. Section 4 discusses boundary conditions paving the way for coupling with circuit models. Then, in section 5, we derive weak formulations. In the final section 6 we will explain how we realized an implementation with finite elements, demonstrate the importance of stabilizing the electro-quasistatic model at the stationary limit, and illuminate the physical interpretation of our two-step procedure.

2. Electromagnetic Models. We first review established frequency-domain models for electromagnetic phenomena, see also [6, 13]. Among them, the quasistatic models are approximations that neglect either inductive or capacitive effects. The static models, however, are true specializations of Maxwell's equations at zero frequency. We write $\omega > 0$ for the fixed angular frequency, and $\imath$ for the imaginary unit. Time domain can be recovered by the replacement $\imath\omega \longrightarrow \partial_t$. We gloss over boundary conditions in this section and postpone their treatment to section 4.

2.1. Full Maxwell's Equations. In a bounded region of space $\Omega \subset \mathbb{R}^3$ we consider Maxwell's equations for linear constitutive material relations and ohmic conductors in frequency domain,

$$\text{(2.1a) Faraday's law:} \qquad \mathbf{curl}\,\mathbf{E} = -\imath\omega\mathbf{B}\,, \quad \operatorname{div}\mathbf{B} = 0\,,$$

$$\text{(2.1b) Ampere's law:} \qquad \mathbf{curl}\,\mathbf{H} = \mathbf{j} + \imath\omega\mathbf{D}\,,$$

$$\text{(2.1c) Gauss's law:} \qquad \operatorname{div}\mathbf{D} = \rho\,,$$

$$\text{(2.1d) material laws:} \qquad \mathbf{D} = \epsilon\mathbf{E}\,, \quad \mathbf{B} = \mu\mathbf{H}\,, \quad \mathbf{j} = \sigma\mathbf{E} + \mathbf{j}^s\,.$$

Herein $\mathbf{E} : \Omega \to \mathbb{C}^3$ denotes the (complex amplitude of the) electric field, $\mathbf{B} : \Omega \to \mathbb{C}^3$ the magnetic field, $\mathbf{D} : \Omega \to \mathbb{C}^3$ the electric displacement field, $\mathbf{H} : \Omega \to \mathbb{C}^3$ the magnetizing field, $\epsilon : \Omega \to \mathbb{R}^+$ the permittivity, $\mu : \Omega \to \mathbb{R}^+$ the permeability, $\sigma : \Omega \to \mathbb{R}_0^+$ the electrical conductivity, and $\mathbf{j} : \Omega \to \mathbb{C}^3$ is the current density. In order to model coils and space charges in the interior of the computational domain we added a prescribed source current $\mathbf{j}^s = \mathbf{j}_0^s + \imath\omega\mathbf{j}_1^s$. It consists of a solenoidal current $\mathbf{j}_0^s : \Omega \to \mathbb{C}^3$, $\operatorname{div}\mathbf{j}_0^s = 0$, for the coils and a fictitious current $\mathbf{j}_1^s : \Omega \to \mathbb{C}^3$ with $\operatorname{div}\mathbf{j}_1^s = -\rho^s$ for a prescribed source charge density $\rho^s : \Omega \to \mathbb{C}$.

At this point let us specify the setting for the considerations in this article, see also Figure 1:

- We assume that the computational domain Ω is partitioned into
  (i) a non-conducting domain (air region) Ω_A where $\sigma = 0$,

(ii) and a conducting domain Ω_C where σ is positive and uniformly bounded away from 0, that is,

$$\overline{\Omega} = \overline{\Omega}_A \cup \overline{\Omega}_C \,, \quad \Omega_A \cap \Omega_C = \emptyset \,,$$

In particular, σ has a non-vanishing jump across $\partial\Omega_C$.

- Source charges can only exist in the non-conducting domain Ω_A, and there Gauss's law reads

$$\operatorname{div} \mathbf{D} = \rho^s \quad \text{in } \Omega_A \,. \tag{2.2}$$

- We take for granted that the exciting current $\mathbf{j}^s$ is supported inside Ω_A: $\operatorname{supp}(\mathbf{j}^s) \subset \Omega_A$.
- We also assume that Ω has trivial topology, that is, no holes and no cavities. The treatment of topologically complex arrangements is elaborated in [8].
- The field model inside Ω is connected to the outside world through *contacts*, also called *electric ports*, which are simply-connected well-separated patches on the boundary of Ω.

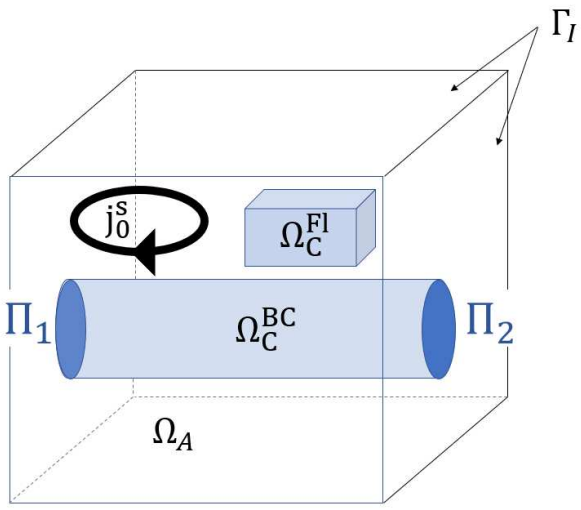

FIG. 1. *Setting with connected conductor Ω_C^{BC}, floating conductor Ω_C^{Fl}, air-domain Ω_A, two contacts Π_1, Π_2, source current $\mathbf{j}_0^s$ supported inside Ω_A, and insulated boundary Γ_I.*

Faraday's law (2.1a) is fulfilled automatically, if electromagnetic potentials, i.e. the electric scalar potential $\varphi : \Omega \to \mathbb{C}$, and the magnetic vector potential $\mathbf{A} : \Omega \to \mathbb{C}^3$ are used to write

$$\mathbf{E} = -\operatorname{\mathbf{grad}} \varphi - \imath\omega\mathbf{A} \,, \quad \mathbf{B} = \operatorname{\mathbf{curl}} \mathbf{A} \,. \tag{2.3}$$

Inserting this approach into Ampère's law (2.1b) yields the ***Full Maxwell Model*** in potential formulation

$$\operatorname{\mathbf{curl}} \frac{1}{\mu} \operatorname{\mathbf{curl}} \mathbf{A} + (\sigma + \imath\omega\epsilon)(\operatorname{\mathbf{grad}} \varphi + \imath\omega\mathbf{A}) = \mathbf{j}^s \,. \tag{2.4}$$

This is an *un-gauged* formulation: Even if we impose appropriate boundary conditions, for every ω (2.4) will fail to possess a unique solution for the potentials $(\mathbf{A}, \varphi)$, though

unique physical fields $\mathbf{E}$ and $\mathbf{B}$ can always be recovered through (2.3). Uniqueness of the potentials can be restored by imposing an additional gauge condition, e.g., the Coulomb gauge $\operatorname{div}\mathbf{A}=0$.

A more sinister *instability* haunts (2.4), the so-called *low-frequency breakdown*: In case $\omega=0$ and $\Omega_A\neq\emptyset$ the electric field $\mathbf{E}$ can no longer be computed from (2.4), because the scalar potential φ becomes undefined in Ω_A. This will, in general, lead to a blow-up of $\mathbf{E}$ as $\omega\to 0$. As a consequence, numerical models based on (2.4) cannot deliver accurate approximations of $\mathbf{E}$ in Ω_A for $\omega\approx 0$. Devising a remedy is a central objective of this work.

2.2. Quasistatic Models. An important approximate model in low-frequency electromagnetics is the ***Magneto-Quasistatic Model*** (or Eddy-Current Model) that results from (2.4) by dropping the displacement field term $\imath\omega\mathbf{D}$ in Ampère's law (2.1b), i.e. by neglecting capacitive effects:

$$\mathbf{curl}\,\frac{1}{\mu}\,\mathbf{curl}\,\mathbf{A}+\sigma\,(\mathbf{grad}\,\varphi+\imath\omega\mathbf{A})=\mathbf{j}_0^s\quad\text{in }\Omega\,. \tag{2.5}$$

The ***Electro-Quasistatic Model (EQS)*** is the second fundamental quasistatic model. It is used when induction can be neglected, assumes $\mathbf{curl}\,\mathbf{E}=0$, and, thus, the electric field can be expressed by the scalar potential φ alone: $\mathbf{E}=-\mathbf{grad}\,\varphi$. By applying the divergence on (2.1b) we infer

$$-\operatorname{div}\left((\sigma+\imath\omega\epsilon)\,\mathbf{grad}\,\varphi\right)=\imath\omega\rho^s\quad\text{in }\Omega\,. \tag{2.6}$$

When endowed with suitable boundary conditions, the solution of this partial differential equation will be unique (maybe only up to a constant). The magnetic field is usually not of interest, when the EQS model is applied. Breakdown in the stationary limit for $\omega=0$ is evident, because in this case the potential becomes undefined in the non-conductive domain Ω_A where $\sigma=0$.

2.3. Static Models. In the case $\omega=0$ one utilizes the following static models for which the electric field can be described by a scalar potential: $\mathbf{E}=-\mathbf{grad}\,\varphi$, see equation (2.3).

- The ***DC-Conduction Model*** is used to compute the ohmic current in conducting domains Ω_C with $\sigma>0$:

$$-\operatorname{div}(\sigma\,\mathbf{grad}\,\varphi)=0\quad\text{in }\Omega_C\,. \tag{2.7}$$

- In the ***Magnetostatic Model*** (with Coulomb gauge) one computes the magnetic field from the current that results from (2.7) by solving

$$\mathbf{curl}\,\frac{1}{\mu}\,\mathbf{curl}\,\mathbf{A}=-\sigma\,\mathbf{grad}\,\varphi+\mathbf{j}_0^s\quad,\quad\operatorname{div}\mathbf{A}=0\quad\text{in }\Omega\,. \tag{2.8}$$

- The ***Electrostatic Model*** is based on Gauss's law (2.1c), complements (2.7), and is used to compute the extension of the electric scalar potential into the non-conducting domain Ω_A with $\sigma=0$

$$-\operatorname{div}(\epsilon\,\mathbf{grad}\,\varphi)=\rho^s\quad\text{in }\Omega_A\,. \tag{2.9}$$

For a related discussion of static models refer to [5, Remark 2].

3. Main Ideas. We introduce the two basic ideas that have inspired this article. Details will be discussed in the following sections.

I. Electro-Quasistatic Gauge. We propose to compute the full-Maxwell solution for $\mathbf{E}$ (and, optionally, for $\mathbf{H}$) in a sequential *two-step procedure*. The first step amounts to solving the electro-quasistatic model. The resulting scalar potential φ serves as a gauge condition for the second step, which, on the one hand, corrects the electric-field for inductive effects, and, on the other hand, is needed to calculate the magnetic field.

- **Step I (EQS)**, *cf.* (2.6): Solve

$$-\operatorname{div}\left((\sigma+\imath\omega\epsilon)\,\mathbf{grad}\,\varphi\right)=\imath\omega\rho^s \quad \text{in } \Omega\,, \tag{3.1}$$

- **Step II (Maxwell)**, *cf.* (2.4): Using φ from (3.1) solve

$$\mathbf{curl}\,\frac{1}{\mu}\,\mathbf{curl}\,\mathbf{A}+(\imath\omega\sigma-\omega^2\epsilon)\mathbf{A}=-(\sigma+\imath\omega\epsilon)\,\mathbf{grad}\,\varphi+\mathbf{j}^s \quad \text{in } \Omega\,. \tag{3.2}$$

Each of the two equations (3.1) and (3.2) has a unique solution for $\omega > 0$, if they are equipped with appropriate boundary conditions, see section 4. Therefore (3.1) can be interpreted as supplying a gauge condition by fixing the scalar potential. Combining (3.1) and (3.2) with $\operatorname{div}\mathbf{j}^s=-\imath\omega\rho^s$ we conclude

$$\operatorname{div}\big((\imath\omega\sigma-\omega^2\epsilon)\mathbf{A}\big)=0 \quad \text{in } \Omega\,. \tag{3.3}$$

The alert reader will have noticed that we lose this implicit gauge condition for the static limit $\omega = 0$: (3.2) will fail to yield a unique solution for $\mathbf{A}$ in this case! Yet, the vector potential $\mathbf{A}$ is not needed for the computation of the electric field in the static case and we just obtain $\mathbf{E}=-\mathbf{grad}\,\varphi$, see (2.3). A unique magnetic induction $\mathbf{B}$ can also be recovered, because any undetermined contribution to $\mathbf{A}$ has vanishing $\mathbf{curl}$ and will not affect $\mathbf{B}=\mathbf{curl}\,\mathbf{A}$.

What about small, but no-zero $\omega > 0$? For $\omega \to 0$ we have to brace for a blow-up of order ω^{-1} of irrotational components of $\mathbf{A}$ inside the conductor Ω_C. Reassuringly, this is just offset by the scaling by ω in $\mathbf{E}=-\mathbf{grad}\,\varphi-\imath\omega\mathbf{A}$. Even if we lose control of parts of $\mathbf{A}$, we retain control of $\mathbf{E}$ in Ω_C! The situation is worse in Ω_A, where $\mathbf{curl}$-free components of $\mathbf{A}$ may explode like $O(\omega^{-2})$ for $\omega \to 0$, and where (3.2) inevitably loses control of $\mathbf{E}$. Undeniably, like (2.4) and (3.1), (3.2) is haunted by low-frequency breakdown in Ω_A! The next section will address a way to overcome it.

II. Generating System Approach For Stabilization. Instability will haunt boundary value problems for the equations (3.1) and (3.2) in the stationary limit $\omega \to 0$. The reason is that for $\omega > 0$ Gauss's law (2.1c) is only implicitly included in equation (3.1), as well as in equation (3.2). Yet, for $\omega = 0$, Gauss's law (2.2) in Ω_A must be enforced separately, because neither of the two equations determines the electric field in the non-conducting domain. In order to balance the numbers of equations and unknowns, it is then required to augment the systems by additional "redundant" unknowns. After Galerkin discretization we end up with a consistent, albeit singular, linear system of equations, which can be solved iteratively. This is the gist of the so-called generating system approach introduced in [7]. We apply it in both steps.

In **Step I (EQS)**, in the case of equation (3.1), we split the potential into two parts $\varphi=\widehat{\varphi}+\psi$, and instead of (3.1) we consider the stabilized version

$$-\operatorname{div}\left((\sigma+i\omega\epsilon)\,\mathbf{grad}(\widehat{\varphi}+\psi)\right)=\imath\omega\rho^s \qquad \text{in} \quad \Omega\,, \tag{3.4a}$$

$$-\operatorname{div}\left(\epsilon\,\mathbf{grad}(\widehat{\varphi}+\psi)\right)=\rho^s \qquad \text{in} \quad \Omega_A\,. \tag{3.4b}$$

The additional potential ψ is constant on every connected component of the conducting region Ω_C. The splitting of φ into $\widehat{\varphi}$ and ψ is not unique, but φ itself remains unique (tacitly assuming suitable boundary conditions).

In **Step II (Maxwell)**, in the case of equation (3.2), we saw that the principal $O(\omega^{-2})$-instability of the vector potential $\mathbf{A}$ for $\omega \to 0$ is caused by vectorfields belonging to the kernel of **curl** and supported in the air region Ω_A. In the generating system approach these have to be represented by one component of a non-unique splitting. Accordingly, we decompose the vector potential as $\mathbf{A} = \widehat{\mathbf{A}} + \mathbf{grad}\,\nu$, where ν is a scalar potential supported in Ω_A. Thus $\mathbf{grad}\,\nu$ takes care of the unstable solution components. Summing up, instead of (3.2) we consider the stabilized version of (3.2)

$$\mathbf{curl}\,\frac{1}{\mu}\,\mathbf{curl}\,\widehat{\mathbf{A}} + (\sigma + \imath\omega\epsilon)\imath\omega(\widehat{\mathbf{A}} + \mathbf{grad}\,\nu) = -(\sigma + \imath\omega\epsilon)\,\mathbf{grad}\,\varphi + \mathbf{j}^s \quad \text{in} \quad \Omega\,, \tag{3.5a}$$

$$\operatorname{div}\Big(\epsilon(\widehat{\mathbf{A}} + \mathbf{grad}\,\nu)\Big) = 0 \quad \text{in} \quad \Omega_A\,. \tag{3.5b}$$

Of course, the splitting of $\mathbf{A}$ into $\widehat{\mathbf{A}}$ and $\mathbf{grad}\,\nu$ is not unique, and (3.5) will fail to possess a unique solution. However, $\mathbf{A}$ itself remains unique for $\omega > 0$, provided that appropriate boundary conditions are imposed, which is the topic of the next section.

4. ECE Boundary Conditions. The possibility to couple the field model to an external circuit through contact surfaces (or ports) is a crucial requirement in low-frequency applications. In a physically sound way this can be done using the so-called electric circuit element (ECE) boundary conditions [3,4,10]. They distinguish contact or port parts of the boundary $\partial\Omega$ and their complement that we call the insulated boundary part Γ_I. For the sake of simplicity, we confine ourselves to a situation with only two contacts $\Pi_1, \Pi_2 \subset \partial\Omega$, as sketched in Figure 1. Refer to [8] for the discussion of more general situations.

The ECE treatment of contacts/electric ports and the insulated boundary Γ_I is based on the following assumptions [4,8]:

(i) There is no inductive coupling with the exterior:

$$\imath\omega\mathbf{B}\cdot\boldsymbol{n} = 0 \quad \Longleftrightarrow \quad \mathbf{curl}\,\mathbf{E}\cdot\boldsymbol{n} = 0 \quad \text{on the entire boundary } \partial\Omega\,,$$

where $\boldsymbol{n}$ is the outer unit normal vectorfield on $\partial\Omega$.

(ii) The contacts are equipotential surfaces: the tangential components $\mathbf{E}_{\boldsymbol{t}}$ of the electric field $\mathbf{E}$ vanish on Π_1 and Π_2.

(iii) No electric currents can penetrate the insulated boundary part:

$$\mathbf{curl}\,\mathbf{H}\cdot\boldsymbol{n} = 0 \quad \Longleftrightarrow \quad \mathbf{E}\cdot\boldsymbol{n} = 0 \quad \text{on } \Gamma_I.$$

From (i) and (ii) we conclude that the tangential component trace $\mathbf{E}_{\boldsymbol{t}} := (\boldsymbol{n}\times\mathbf{E})\times\boldsymbol{n}|_{\partial\Omega}$ of the electric field $\mathbf{E}$ at the boundary is the surface gradient of a scalar potential $\partial\Omega \to \mathbb{R}$ that is constant on each contact:

$$\mathbf{E}_{\boldsymbol{t}} = \mathbf{grad}_\Gamma\left(\varphi_{\mathrm{tot}}|_{\partial\Omega}\right)\,, \tag{4.1}$$

for some

$$\varphi_{\mathrm{tot}} \in H^1_{\mathrm{ece}}(\Omega) := \left\{ \phi : \Omega \to \mathbb{R} : \begin{array}{l} \phi \in H^1(\Omega)\,, \\ \phi|_{\Pi_j} \equiv \text{ const}, \, j = 1,2 \end{array} \right\}\,. \tag{4.2}$$

Here, we wrote $H^1(\Omega)$ for the classical Sobolev space of square integrable complex-valued functions with square integrable gradients.

Voltages $U_{m,n}$ between two contacts Π_m and Π_n, and the current I_m through the contact Π_m are the principal port quantities for field-circuit coupling. They are readily available from ECE boundary condition through the formulas

$$U_{m,n} := V_m - V_n \text{ , where } \quad V_m := \phi|_{\Pi_m} \ , \quad V_n := \phi|_{\Pi_n} \ , \tag{4.3}$$

$$I_m := \int_{\Pi_m} \mathbf{curl}\,\mathbf{H} \cdot \boldsymbol{n}\,\mathrm{d}S \ . \tag{4.4}$$

Obviously, all electromagnetic effects, resistive, capacitive, and inductive, contribute to the voltage drops between contacts, and to the currents through contacts. Therefore, in our approach both **Step I** and **Step II** will contribute to the port quantities. This has an added benefit, because it makes possible to separate

(i) the capacitive/resistive contributions $U_{\mathrm{stat},m,n}$ and $I_{\mathrm{stat},m}$, that will be solely determined in **Step I** from

(ii) the inductive contributions $U_{\mathrm{ind},m,n}$ and $I_{\mathrm{ind},m}$, that will be calculated in **Step II**.

They add up to the total voltages and currents:

$$U_{m,n} = U_{\mathrm{stat},m,n} + U_{\mathrm{ind},m,n} \ , \tag{4.5}$$

$$I_m = I_{\mathrm{stat},m} + I_{\mathrm{ind},m} \ . \tag{4.6}$$

It turns out that the ECE port boundary conditions (i)-(iii) neatly fit our approach and can be applied in both steps:

(I) In **Step I (EQS)** in (3.1) we compute a scalar potential φ anyway, and thus fulfill condition (i). We choose $\varphi \in H^1_{\mathrm{ece}}(\Omega)$, which amounts to imposing a constant potential at contacts according to condition (ii)

$$\varphi|_{\Pi_j} \equiv \text{const} \ , \quad j = 1, 2 \ , \tag{4.7}$$

to be complemented by the zero-current condition (iii) on the insulated boundary part

$$(\sigma + \imath\omega\epsilon)\,\mathbf{grad}\,\varphi \cdot \boldsymbol{n} = 0 \quad \text{on } \Gamma_I \ . \tag{4.8}$$

We remind that in the electro-quasistatic model the "(quasi)static" currents through the contacts are accessible through the flux integrals

$$I_{\mathrm{stat},\,j} := -\int_{\Pi_j} (\sigma + \imath\omega\epsilon)\,\mathbf{grad}\,\varphi \cdot \boldsymbol{n}\,\mathrm{d}S \ , \quad j = 1, 2 \ . \tag{4.9}$$

We point out that the divergence theorem applied to (3.1) yields the flux balance condition

$$I_{\mathrm{stat},1} + I_{\mathrm{stat},2} = \imath\omega \int_\Omega \rho^s \,\mathrm{d}\mathbf{x} \ . \tag{4.10}$$

(II) In order to ensure (4.1) in light of (2.3), for the solution $\mathbf{A}$ of (3.2) in **Step II (Maxwell)** we have to demand that the tangential component trace $\mathbf{A}_t$ of the vector potential $\mathbf{A}$ is the surface gradient of another scalar potential

$$\mathbf{A}_t = \mathbf{grad}_\Gamma\, \eta_{\mathbf{A}}|_{\partial\Omega} \quad \text{on } \partial\Omega \quad \text{for some} \quad \eta_{\mathbf{A}} \in H^1_{\mathrm{ece}}(\Omega) \ , \tag{4.11}$$

with $H^1_{\mathrm{ece}}(\Omega)$ as in (4.2). We point out that $\mathbf{A}_{\boldsymbol{t}}$ fixes $\eta_{\mathbf{A}}|_{\partial\Omega}$ up to a constant. Since we have assumed trivial topology of Ω this is *equivalent* to imposing $\mathbf{B}\cdot\boldsymbol{n}=0$ on the entire boundary, i.e. condition (i), and to enforce vanishing tangential components of $\mathbf{A}$ on contacts, i.e. condition (ii):

$$(4.11) \iff \begin{cases} \mathbf{curl}\,\mathbf{A}\cdot\boldsymbol{n} &= 0 \quad \text{on } \partial\Omega\,, \\ \mathbf{A}_{\boldsymbol{t}} &= 0 \quad \text{on } \Gamma_1\cup\Gamma_2\,. \end{cases} \tag{4.12}$$

More explicitly, the scalar surface potential $\eta_{\mathbf{A}}$ in (4.11) has to satisfy boundary conditions (ii) that mirror (4.7):

$$\eta_{\mathbf{A}}|_{\Gamma_j} \equiv \text{const}\,, \quad j=1,2\,, \tag{4.13}$$

The counterpart of (4.8) is the zero-current condition (iii) on the insulated boundary part expressed as ($\mathbf{H}=\mu^{-1}\,\mathbf{curl}\,\mathbf{A}$)

$$\mathrm{div}_\Gamma\big(\frac{1}{\mu}\,\mathbf{curl}\,\mathbf{A}\times\boldsymbol{n}\big) = \mathrm{div}_\Gamma\big(\mathbf{H}\times\boldsymbol{n}\big) = \mathbf{curl}\,\mathbf{H}\cdot\boldsymbol{n} = 0 \quad \text{on } \Gamma_I\,. \tag{4.14}$$

Remark 4.1. We recover the "inductive" current contribution of Step II as

$$I_{\mathrm{ind},\,j} := -\imath\omega\int_{\Gamma_j}(\sigma+\imath\omega\epsilon)\mathbf{A}\cdot\boldsymbol{n}\,\mathrm{d}S\,, \quad j=1,2\,. \tag{4.15}$$

From (3.2) we conclude $\mathrm{div}((\sigma+\imath\omega)\mathbf{A})=0$, *cf.* (3.3), which implies balance of induced currents:

$$I_{\mathrm{ind},1}+I_{\mathrm{ind},2}=0\,. \tag{4.16}$$

By (2.3) the total scalar boundary potential $\varphi_{\mathrm{tot}}|_{\partial\Omega}$ from (4.1) is a superposition of the scalar potentials obtained in both steps

$$\varphi_{\mathrm{tot}}|_{\partial\Omega} = \varphi|_{\partial\Omega} + \imath\omega\,\eta_{\mathbf{A}}|_{\partial\Omega}\,, \quad \begin{cases} \varphi \text{ from Step I,} \\ \eta_{\mathbf{A}} \text{ from Step II,} \end{cases} \tag{4.17}$$

so that the total voltage drop between two contacts can be computed as

$$U_{1,2} = \underbrace{\varphi|_{\Gamma_2}-\varphi|_{\Gamma_1}}_{=:\,U_{\mathrm{stat},1,2}} + \underbrace{\imath\omega\big(\,\eta_{\mathbf{A}}|_{\Gamma_2}-\eta_{\mathbf{A}}|_{\Gamma_1}\,\big)}_{=:\,U_{\mathrm{ind},1,2}}\,. \tag{4.18}$$

Analogously, the currents (4.9) and (4.15) add up to the total current flowing through a contact:

$$I_j = \underbrace{-\int_{\Gamma_j}(\sigma+\imath\omega\epsilon)\,\mathbf{grad}\,\varphi\cdot\boldsymbol{n}\,\mathrm{d}S}_{=:\,I_{\mathrm{stat},\,j}} \underbrace{-\imath\omega\int_{\Gamma_j}(\sigma+\imath\omega\epsilon)\mathbf{A}\cdot\boldsymbol{n}\,\mathrm{d}S}_{=:\,I_{\mathrm{ind},\,j}}\,, \quad j=1,2\,. \tag{4.19}$$

Summing up, all port quantities comprise two contributions: one due to electroquasistatic effects that are solely determined in Step I, the other representing an inductive correction that is determined in Step II.

Remark 4.2. Combining (4.10) and (4.16) yields a constraint on the contact currents:

$$I_1+I_2 = I_{\mathrm{stat},1}+I_{\mathrm{ind},1}+I_{\mathrm{stat},2}+I_{\mathrm{ind},2} = \imath\omega\int_\Omega \rho^s\,\mathrm{d}\mathbf{x}\,. \tag{4.20}$$

Further, in the static case $\omega=0$ non-zero contact currents can only be imposed at contacts connected to the conducting region Ω_C.

5. Variational (Weak) Formulations. In this section we present variational formulations for the boundary value problems to be solved in Step I (EQS) and Step II (Maxwell) of our approach. They are the starting point for finite-element discretization, see subsection 6.1. We use the ECE port boundary conditions introduced above, and, as in section 4, restrict ourselves to the two-port setting with contacts Π_1 and Π_2. All the other assumptions made in section 3 still apply, see Figure 1 for a typical situation.

5.1. Step I (EQS): Weak Formulations.

5.1.1. Standard Electro-Quasistatics (EQS). As already mentioned in section 4, the ECE boundary conditions (4.1) for (3.1) are captured by representing the electric scalar potential as

$$\varphi = \widetilde{\varphi} + V_{\mathrm{stat},1}\Phi_1 + V_{\mathrm{stat},2}\Phi_2 \ ,$$

and enriching the function space

$$H^1_{\mathrm{ece},0}(\Omega) := \left\{ \psi \in H^1(\Omega) : \ \psi|_{\Pi_j} = 0 \ , \ j = 1,2 \right\} \ , \tag{5.1}$$

of admissible scalar potentials $\widetilde{\varphi}$ with the *offset functions*

$$\Phi_1,\, \Phi_2 \in H^1_{\mathrm{ece}}(\Omega) \ , \quad \Phi_1|_{\Pi_1} = 1, \ \Phi_1|_{\Pi_2} \equiv 0 \ , \quad \Phi_2|_{\Pi_1} \equiv 0, \ \Phi_2|_{\Pi_2} = 1 \ , \tag{5.2}$$

that can be chosen to have localized support at the ports. Integration by parts, by applying Green's formula to (3.1), together with the zero-current boundary condition (4.8), and the current formula (4.9), yield the variational problem: seek $\widetilde{\varphi} \in H^1_{\mathrm{ece},0}(\Omega)$, $V_{\mathrm{stat},1}, V_{\mathrm{stat},2} \in \mathbb{C}$, such that

$$\begin{aligned} \int_\Omega (\sigma + \imath\omega\epsilon)\, \mathbf{grad}(\widetilde{\varphi} + V_{\mathrm{stat},1}\Phi_1 + V_{\mathrm{stat},2}\Phi_2) \cdot \mathbf{grad}\, \widetilde{\varphi}' \,\mathrm{d}\mathbf{x} \\ = \imath\omega \int_\Omega \rho^s \widetilde{\varphi}' \,\mathrm{d}\mathbf{x} \ , \end{aligned} \tag{5.3a}$$

$$\begin{aligned} \int_\Omega (\sigma + \imath\omega\epsilon)\, \mathbf{grad}(\widetilde{\varphi} + V_{\mathrm{stat},1}\Phi_1 + V_{\mathrm{stat},2}\Phi_2) \cdot \mathbf{grad}\, \Phi_j \,\mathrm{d}\mathbf{x} \\ = -I_{\mathrm{stat},j} + \imath\omega \int_\Omega \rho^s \Phi_j \,\mathrm{d}\mathbf{x} \end{aligned} \tag{5.3b}$$

for all $\widetilde{\varphi}' \in H^1_{\mathrm{ece},0}(\Omega)$ and $j = 1, 2$.

The static voltage between the two ports is given by $U_{\mathrm{stat},1,2} = V_{\mathrm{stat},2} - V_{\mathrm{stat},1}$. The currents $I_{\mathrm{stat},1}$ and $I_{\mathrm{stat},2}$ that flow through the ports Π_1 and Π_2 fulfill (4.10), as can be seen by testing (5.3) with $\widetilde{\varphi}' := 1 - \Phi_1 - \Phi_2 \in H^1_{\mathrm{ece},0}(\Omega)$, and adding all three equations.

5.1.2. Stabilized Electro-Quasistatics (SEQS). The variational problem suffers instability for $\omega \to 0$, as we lose control of φ in the non-conducting region Ω_A where $\sigma \equiv 0$. As mentioned in section 3, this can be remedied by the generating system approach according to (3.4). Its weak formulation extends (5.3) and relies on the additional function space $H^1_e(\Omega)$, which includes those functions in $H^1_{\mathrm{ece}}(\Omega)$ that are constant in floating conductors and that vanish in conductors that are connected to a port

$$H^1_e(\Omega) := \left\{ \begin{array}{l} \psi \in H^1_{\mathrm{ece},0}(\Omega) \quad (\text{, that is } \psi|_{\Pi_1} = \psi|_{\Pi_2} = 0) \ , \\ \psi \equiv \text{const on all connected components of } \Omega_C \end{array} \right\} \ . \tag{5.4}$$

Following [7], we add a function $\psi \in H^1_e(\Omega)$ to the trial and test functions of (5.3), represent the electric scalar potential as

$$\varphi = \underbrace{\widehat{\varphi} + \psi}_{=\widetilde{\varphi}} + V_{\mathrm{stat},1}\Phi_1 + V_{\mathrm{stat},2}\Phi_2 \in H^1_{\mathrm{ece}}(\Omega)\ , \tag{5.5}$$

and arrive at the following singular variational problem.

SEQS problem: seek $\widehat{\varphi} \in H^1_{\mathrm{ece},0}(\Omega)$, $\psi \in H^1_e(\Omega)$, $V_{\mathrm{stat},1}, V_{\mathrm{stat},2} \in \mathbb{C}$ such that

$$\begin{aligned}\int_\Omega (\sigma + \imath\omega\epsilon)\,\mathbf{grad}(\widehat{\varphi} + \psi + V_{\mathrm{stat},1}\Phi_1 + V_{\mathrm{stat},2}\Phi_2)\cdot\mathbf{grad}\,\widehat{\varphi}'\,\mathrm{d}\mathbf{x} \\ = \imath\omega\int_\Omega \rho^s\widehat{\varphi}'\,\mathrm{d}\mathbf{x}\ ,\end{aligned} \tag{5.6a}$$

$$\begin{aligned}\int_{\Omega_A} \epsilon\,\mathbf{grad}(\widehat{\varphi} + \psi + V_{\mathrm{stat},1}\Phi_1 + V_{\mathrm{stat},2}\Phi_2)\cdot\mathbf{grad}\,\psi'\,\mathrm{d}\mathbf{x} \\ = \int_\Omega \rho^s\,\psi'\,\mathrm{d}\mathbf{x}\ ,\end{aligned} \tag{5.6b}$$

$$\begin{aligned}\int_\Omega (\sigma + \imath\omega\epsilon)\,\mathbf{grad}(\widehat{\varphi} + \psi + V_{\mathrm{stat},1}\Phi_1 + V_{\mathrm{stat},2}\Phi_2)\cdot\mathbf{grad}\,\Phi_j\,\mathrm{d}\mathbf{x} \\ = -I_{\mathrm{stat},j} + \imath\omega\int_\Omega \rho^s\Phi_j\,\mathrm{d}\mathbf{x}\end{aligned} \tag{5.6c}$$

for all $\widehat{\varphi}' \in H^1_{\mathrm{ece},0}(\Omega)$, $\psi' \in H^1_e(\Omega)$, $j = 1, 2$.

By "singular" we mean that the bilinear form underlying (5.6) has a non-trivial null space: Setting $\widehat{\varphi} = -\psi$ for any $\psi \in H^1_e(\Omega)$ gives an element of that null space. However, thanks to the consistency of the right-hand side it possesses solutions $\widehat{\varphi}, \psi$. From those we recover a unique (up to a constant) electric scalar potential φ, which agrees with the φ obtained in subsection 5.1.1. We also point out that charge neutrality is guaranteed by the choice of H^1_e and equation (5.6b), see [7].

5.2. Step II (Maxwell): Weak Formulations.

5.2.1. Standard A-based Formulation. The ECE boundary conditions manifest themselves as the constraint (4.11) on the magnetic vector potential. This suggests that we represent the magnetic vector potential as $\mathbf{A} = \widetilde{\mathbf{A}} + V_{\mathrm{ind},1}\,\mathbf{grad}\,\Phi_1 + V_{\mathrm{ind},2}\,\mathbf{grad}\,\Phi_2$ and choose $\widetilde{\mathbf{A}}$ from the following function space:

$$\boldsymbol{H}_{\mathrm{ece},0}(\mathbf{curl},\Omega) := \left\{ \mathbf{v} \in \boldsymbol{H}(\mathbf{curl},\Omega) : \begin{array}{l} \text{there is } \eta_{\mathbf{v}} \in H^1_{\mathrm{ece},0}(\Omega) : \\ \mathbf{v}_{\boldsymbol{t}} = \mathbf{grad}\,(\eta_{\mathbf{v}}|_{\partial\Omega}) \text{ on } \partial\Omega \end{array} \right\}\ , \tag{5.7}$$

see (5.1) for the definition of $H^1_{\mathrm{ece},0}(\Omega)$. This needs explaining: First recall that the function space $\boldsymbol{H}(\mathbf{curl},\Omega)$ contains square-integrable vectorfields, whose **curl** is square-integrable as well. It is the natural space for electromagnetic fields with finite energy. Second, as before, a subscript $\boldsymbol{t}$ designates the tangential component of a vectorfield on $\partial\Omega$. Hence, functions belonging to $\boldsymbol{H}_{\mathrm{ece},0}(\mathbf{curl},\Omega)$ have vanishing tangential components on all contacts, *cf.* (4.12). Moreover, their tangential components on all of $\partial\Omega$ can be written as the surface gradient of a scalar potential, *cf.* (4.11). Thus functions $\widetilde{\mathbf{A}}$ in the space $\boldsymbol{H}_{\mathrm{ece},0}(\mathbf{curl},\Omega)$ can be represented as

$$\widetilde{\mathbf{A}} = \mathbf{A}_0 + \mathbf{grad}\,\eta_{\mathbf{v}}\ , \tag{5.8}$$

where $\mathbf{A}_0 \in \boldsymbol{H}(\mathbf{curl},\Omega)$ has vanishing tangential trace on $\partial\Omega$ and $\eta_{\mathbf{v}} \in H^1_{\mathrm{ece},0}(\Omega)$. We must not forget to add gradients of offset functions to $\boldsymbol{H}_{\mathrm{ece},0}(\mathbf{curl},\Omega)$, since in (5.7) the surface gradients are restricted to $H^1_{\mathrm{ece},0}(\Omega)\big|_{\partial\Omega}$; as ultimate trial space we rely on $\boldsymbol{H}_{\mathrm{ece},0}(\mathbf{curl},\Omega) + \mathrm{Span}\,\{\mathbf{grad}\,\Phi_1, \mathbf{grad}\,\Phi_2\}$.

Next, using Green's formula for **curl** on (3.2) and taking into account the boundary conditions gives the variational formulation: seek $\widetilde{\mathbf{A}} \in \boldsymbol{H}_{\mathrm{ece},0}(\mathbf{curl},\Omega)$, $V_{\mathrm{ind},1}, V_{\mathrm{ind},2} \in \mathbb{C}$, such that

$$\int_\Omega \mu^{-1}\,\mathbf{curl}\,\widetilde{\mathbf{A}}\cdot\mathbf{curl}\,\widetilde{\mathbf{A}}'\,\mathrm{d}\mathbf{x} + \int_\Omega (\sigma+\imath\omega\epsilon)\imath\omega(\widetilde{\mathbf{A}} + V_{\mathrm{ind},1}\,\mathbf{grad}\,\Phi_1 + V_{\mathrm{ind},2}\,\mathbf{grad}\,\Phi_2)\cdot\widetilde{\mathbf{A}}'\,\mathrm{d}\mathbf{x} = \int_\Omega \big(-(\sigma+\imath\omega\epsilon)\,\mathbf{grad}\,\varphi + \mathbf{j}^s\big)\cdot\widetilde{\mathbf{A}}'\,\mathrm{d}\mathbf{x}\,, \tag{5.9a}$$

$$\int_\Omega (\sigma+\imath\omega\epsilon)\imath\omega(\widetilde{\mathbf{A}} + V_{\mathrm{ind},1}\,\mathbf{grad}\,\Phi_1 + V_{\mathrm{ind},2}\,\mathbf{grad}\,\Phi_2)\cdot\mathbf{grad}\,\Phi_j\,\mathrm{d}\mathbf{x} = -I_{\mathrm{ind},j}\,. \tag{5.9b}$$

for all $\widetilde{\mathbf{A}}' \in \boldsymbol{H}_{\mathrm{ece},0}(\mathbf{curl},\Omega)$.

The induced voltage between the contacts is $U_{\mathrm{ind},1,2} = \imath\omega(V_{\mathrm{ind},2} - V_{\mathrm{ind},1})$. The inductive currents flowing through Π_1 and Π_2 directly enter as $I_{\mathrm{ind},1}$ and $I_{\mathrm{ind},2}$. Adding all three equations with $\widetilde{\mathbf{A}}' := \mathbf{grad}(1-\Phi_1-\Phi_2) \in \boldsymbol{H}_{\mathrm{ece},0}(\mathbf{curl},\Omega)$ confirms the flux balance law (4.16).

5.2.2. Stabilized A-Based Formulation. As explained in section 3 we augment (5.9) with gradients of scalar potentials ν supported in Ω_A as "redundant" unkowns. This means that we write

$$\mathbf{A} = \underbrace{\widehat{\mathbf{A}} + \mathbf{grad}\,\nu}_{=\widetilde{\mathbf{A}}} + V_{\mathrm{ind},1}\,\mathbf{grad}\,\Phi_1 + V_{\mathrm{ind},2}\,\mathbf{grad}\,\Phi_2\,, \tag{5.10}$$

with $\widehat{\mathbf{A}} \in \boldsymbol{H}_{\mathrm{ece},0}(\mathbf{curl},\Omega)$, $\nu \in H^1_C(\Omega)$, and

$$H^1_C(\Omega) := \big\{\ \nu \in H^1_{\mathrm{ece},0}(\Omega) :\ \nu \equiv 0 \text{ on } \Omega_C\ \big\}\,. \tag{5.11}$$

Of course, this splitting is not unique, because $\boldsymbol{H}_{\mathrm{ece},0}(\mathbf{curl},\Omega) + \mathbf{grad}\,H^1_C(\Omega)$ is not a direct sum. Yet, the gradient contribution captures that part of the kernel of **curl** of which we lose control as $\omega \to 0$. Thus, (5.10) turns out to be the right starting point for the generating system approach (3.5) in a variational context. We arrive at the following underdetermined variational problem:

Stabilized Maxwell problem: seek $\widehat{\mathbf{A}} \in \boldsymbol{H}_{\mathrm{ece},0}(\mathbf{curl},\Omega)$, $\nu \in H^1_C(\Omega)$, $V_{\mathrm{ind},1}, V_{\mathrm{ind},2} \in \mathbb{C}$ such that

$$\begin{aligned}
&\int_\Omega \mu^{-1}\,\mathbf{curl}\,\widehat{\mathbf{A}}\cdot\mathbf{curl}\,\widehat{\mathbf{A}}'\,\mathrm{d}\mathbf{x}\\
&+\int_\Omega (\sigma+\imath\omega\epsilon)\imath\omega(\widehat{\mathbf{A}}+\mathbf{grad}\,\nu+V_{\mathrm{ind},1}\,\mathbf{grad}\,\Phi_1+V_{\mathrm{ind},2}\,\mathbf{grad}\,\Phi_2)\cdot\widehat{\mathbf{A}}'\,\mathrm{d}\mathbf{x}\\
&\qquad=\int_\Omega \big(-(\sigma+\imath\omega\epsilon)\,\mathbf{grad}\,\varphi+\mathbf{j}^s\big)\cdot\widehat{\mathbf{A}}'\,\mathrm{d}\mathbf{x}
\end{aligned} \tag{5.12a}$$

$$\int_{\Omega_A} \epsilon(\widehat{\mathbf{A}}+\mathbf{grad}\,\nu+V_{\mathrm{ind},1}\,\mathbf{grad}\,\Phi_1+V_{\mathrm{ind},2}\,\mathbf{grad}\,\Phi_2)\cdot\mathbf{grad}\,\nu'\,\mathrm{d}\mathbf{x}=0\,, \tag{5.12b}$$

$$\begin{aligned}
&\int_\Omega (\sigma+\imath\omega\epsilon)\imath\omega(\widehat{\mathbf{A}}+\mathbf{grad}\,\nu+V_{\mathrm{ind},1}\,\mathbf{grad}\,\Phi_1+V_{\mathrm{ind},2}\,\mathbf{grad}\,\Phi_2)\cdot\\
&\qquad\qquad\mathbf{grad}\,\Phi_j\,\mathrm{d}\mathbf{x}=-I_{\mathrm{ind},j}\,.
\end{aligned} \tag{5.12c}$$

for all $\widehat{\mathbf{A}}' \in \boldsymbol{H}_{\mathrm{ece},0}(\mathbf{curl},\Omega)$, $\nu' \in H^1_C(\Omega)$, $j=1,2$.

5.3. Coupling With Circuits. Let us suppose we want to impose a prescribed voltage between the contacts or a prescribed current through the contacts in the setting of Figure 1. To begin with, recall that according to section 4 both voltages and currents consist of an electro(-quasi)static part that is determined in Step I, and an induced part that is calculated in Step II. In general, excitation through contacts can be imposed in both steps. Imposing a voltage or a current in the second step however thwarts our aim to separate capacitive/resistive contributions from inductive contributions. This can be understood by the following considerations: let us assume we want to impose a voltage U_0. According to Formula (4.18)

$$U_{1,2}=\underbrace{V_{\mathrm{stat},2}-V_{\mathrm{stat},1}}_{=:U_{\mathrm{stat},1,2}}+\underbrace{\imath\omega\big(V_{\mathrm{ind},2}-V_{\mathrm{ind},1}\big)}_{=:U_{\mathrm{ind},1,2}}\,. \tag{5.13}$$

we can calculate a solution φ_1 (in **Step I, EQS**), $\mathbf{A}_1$ (in **Step II, Maxwell**) for the choice $U_{\mathrm{stat},1,2}=U_0$, $U_{\mathrm{ind},1,2}=0$. Alternatively we could also impose $U_{\mathrm{stat},1,2}=0$, $U_{\mathrm{ind},1,2}=U_0$ and obtain the **Step-I** solution $\varphi_2=0$ and the **Step-II** solution $\mathbf{A}_2=\mathbf{A}_1+\frac{1}{\imath\omega}\,\mathbf{grad}\,\varphi_1$. Thus imposing the voltage in Step II leads to the same solution for the electromagnetic fields $\mathbf{E}$ and $\mathbf{H}$, but the entire field, including the capacitive part, is described by the magnetic vector potential. This is not what we intend to do, and in addition leads to problems in the static limit $\omega=0$. Remember how one tackles the static models of subsection 2.3:

(i) One first solves the DC conduction model (2.7) with imposed voltages and currents,
(ii) and then uses the obtained potential as input for magnetostatics (2.8), or electrostatics (2.9).

The DC conduction model is contained in the stabilized electro-quasistatic variational problem (5.6). This motivated our decision that *exciting voltages and currents are generally imposed in Step I (SEQS).*

5.3.1. Current Excitation. We prescribe a current I_1 at Π_1, and fix the potential V_2 at Π_2 to ensure uniqueness of the electric scalar potential.

1. In (5.6) (Step I, SEQS) we fix $I_{\mathrm{stat},1}:=I_1$ and $V_{\mathrm{stat},2}:=V_2$ and drop the equation belonging to Φ_2 from (5.6c).

2. In (5.12) (Step II, Stabilized Maxwell) we set $I_{\mathrm{ind},1} = 0$ and $V_{\mathrm{ind},2} := 0$, and drop the equation belonging to Φ_2 from (5.12c).

The total voltage drop between Π_2 and Π_1 is then given by Formula (5.13).

5.3.2. Voltage Excitation. To impose prescribed potentials $V_2, V_1 \in \mathbb{C}$ at Π_2 and Π_1,

(I) in (5.6) (Step I, SEQS) we fix $V_{\mathrm{stat},1} := V_1$ and $V_{\mathrm{stat},2} := V_2$ and drop the two equations (5.6c).

(II) in (5.12) (Step II, Stabilized Maxwell) we set $V_{\mathrm{ind},1} := 0$ and $V_{\mathrm{ind},2} := 0$ and keep only (5.12a) and (5.12b).

The currents through the contacts can be determined in a post-processing step from (5.6c) (static/capacitive current) and (5.12c) (inductive current) and, then, summing up $I_{\mathrm{stat},j}$ and $I_{\mathrm{ind},j}$, $j = 1, 2$, according to (4.19).

5.3.3. Imposing U-I Relationship. A simple two-port circuit can implicitly be characterized by a voltage-current relationship $F(U_{1,2}, I_2) = 0$ with a function $F : \mathbb{R} \times \mathbb{R} \to \mathbb{R}$. Attaching such a circuit to the two ports Π_2 and Π_1 of the field domain can be done as follows:

1. Augment (5.6) by the additional equation $F(U_{\mathrm{stat},1,2}, I_{\mathrm{stat},2}) = 0$, and solve the resulting variational problem (Step I, SEQS).
2. Then add the extra equation

$$F(U_{\mathrm{stat},1,2} + U_{\mathrm{ind},1,2}, I_{\mathrm{stat},2} + I_{\mathrm{ind},2}) = 0$$

to (5.12) and solve the resulting extended variational problem (Step II, Stabilized Maxwell).

5.3.4. Power Balance. Physically meaningful port potentials and currents must satisfy a power balance relationship. To verify it for our two-step approach, we first find an expression for the contact currents I_j for $\omega > 0$, relying on the variational formulations (5.3) (Step I, QES) and (5.9) (Step II, Maxwell). Stabilization does not matter for the considerations in this section. The total current through contact Π_j can be recast as

$$I_j = I_{\mathrm{stat},j} + I_{\mathrm{ind},j}$$

and continuing with (5.3b) and (5.9b)

$$\begin{aligned} &= -\int_\Omega (\sigma + \imath\omega\epsilon)\, \mathbf{grad}\, \varphi \cdot \mathbf{grad}\, \Phi_j \,\mathrm{d}\mathbf{x} + \imath\omega \int_\Omega \rho^s \Phi_j \,\mathrm{d}\mathbf{x} \\ &\quad - \int_\Omega (\sigma + \imath\omega\epsilon)\imath\omega \mathbf{A} \cdot \mathbf{grad}\, \Phi_j \,\mathrm{d}\mathbf{x} \end{aligned}$$

and with (2.3),

$$= \int_\Omega (\sigma + \imath\omega\epsilon)\mathbf{E} \cdot \mathbf{grad}\, \Phi_j \,\mathrm{d}\mathbf{x} + \imath\omega \int_\Omega \rho^s \Phi_j \,\mathrm{d}\mathbf{x}$$

and with Ampere's law (2.1b),

$$= \int_\Omega (\mathbf{curl}\, \mathbf{H} - \mathbf{j}^s) \cdot \mathbf{grad}\, \Phi_j \,\mathrm{d}\mathbf{x} + \imath\omega \int_\Omega \rho^s \Phi_j \,\mathrm{d}\mathbf{x},$$

and using Green's formula plus the cancellation due to $\operatorname{div}\mathbf{j}^s = -\imath\omega\rho^s$,

$$= \int_{\partial\Omega} \mathbf{curl}\,\mathbf{H}\cdot\boldsymbol{n}\ \Phi_j|_{\partial\Omega}\,\mathrm{d}S\,.$$

Owing to the zero-current condition (4.14), which implies

$$\int_{\partial\Omega} \mathbf{curl}\,\mathbf{H}\cdot\boldsymbol{n}\ \varphi'|_{\partial\Omega}\,\mathrm{d}S = \int_{\partial\Omega} \operatorname{div}_\Gamma(\mathbf{H}\times\boldsymbol{n})\ \varphi'|_{\partial\Omega}\,\mathrm{d}S = 0 \quad \forall\varphi' \in H^1_{\mathrm{ece},0}(\Omega)\,,$$

we can deduce, with $\varphi_{\mathrm{tot}}|_{\partial\Omega} = \varphi|_{\partial\Omega} + \imath\omega\ \eta_{\mathbf{A}}|_{\partial\Omega}$ the scalar surface potential for $\mathbf{E}$ as introduced in (4.1) and (4.17),

$$\begin{aligned} I_1V_1 + I_2V_2 &= \int_{\partial\Omega} \mathbf{curl}\,\mathbf{H}\cdot\boldsymbol{n}\ (V_1\Phi_1 + V_2\Phi_2)|_{\partial\Omega}\,\mathrm{d}S = \int_{\partial\Omega} \mathbf{curl}\,\mathbf{H}\cdot\boldsymbol{n}\ \varphi_{\mathrm{tot}}|_{\partial\Omega}\,\mathrm{d}S \\ &= \int_{\partial\Omega} \operatorname{div}_\Gamma(\mathbf{H}\times\boldsymbol{n})\ \varphi_{\mathrm{tot}}|_{\partial\Omega}\,\mathrm{d}S = -\int_{\partial\Omega} (\mathbf{H}\times\boldsymbol{n})\cdot\mathbf{grad}_\Gamma\ \varphi_{\mathrm{tot}}|_{\partial\Omega}\,\mathrm{d}S \\ &= \int_{\partial\Omega} (\mathbf{H}\times\boldsymbol{n})\cdot\mathbf{E}_{\boldsymbol{t}}\,\mathrm{d}S = \int_{\partial\Omega} (\mathbf{E}\times\mathbf{H})\cdot\boldsymbol{n}\,\mathrm{d}S\,. \end{aligned}$$

The port quantities V_j and I_j provide the electromagnetic power flux through $\partial\Omega$ as given by Poynting's theorem. Thus, in the case $\mathbf{j}^s = 0$ the power P that is transferred to the system is, as expected,

$$\begin{aligned} P &= -\int_{\partial\Omega} (\mathbf{E}\times\mathbf{H})\cdot\boldsymbol{n}\,\mathrm{d}S = \int_\Omega (\mathbf{j}\cdot\mathbf{E} + \imath\omega\,(\mathbf{D}\cdot\mathbf{E} + \mathbf{H}\cdot\mathbf{B}))\ \mathrm{d}\mathbf{x} \\ &= -\big(I_1V_1 + I_2V_2\big) = \big(V_2 - V_1\big)\,I_1 = U_{1,2}I_1\,. \end{aligned}$$

6. Numerical Tests.

6.1. Finite-Element Galerkin Discretization. The computations of this section were carried out on meshes that consisted of curved tetrahedral elements. We used first order piecewise linear Lagrangian ("nodal") finite elements for test and trial functions in $H^1(\Omega)$, and lowest-order edge elements for test and trial functions in $\boldsymbol{H}(\mathbf{curl},\Omega)$. The offset function Φ_j at port j was implemented as piecewise linear nodal finite-element function by setting all its nodal values on port Π_j to 1, and all other nodal values zero. The functions $\widetilde{\mathbf{A}}$ of $\boldsymbol{H}_{\mathrm{ece},0}(\mathbf{curl},\Omega)$, see (5.7), were realized by splitting $\widetilde{\mathbf{A}} = \mathbf{A}_0 + \mathbf{grad}\,\eta_{\mathbf{A}}$ into an interior part $\mathbf{A}_0 \in \boldsymbol{H}(\mathbf{curl},\Omega)$ with vanishing tangential trace $\mathbf{A}_0\times\boldsymbol{n} = 0$ on the boundary $\partial\Omega$, and a part $\mathbf{grad}\,\eta_{\mathbf{A}}$ with $\eta_{\mathbf{A}} \in H^1_{\mathrm{ece},0}(\Omega)$ belonging to the piecewise linear nodal finite-element space with all its nodal values set to zero except those on $\partial\Omega$. Of course, all edge degrees of freedom for $\mathbf{A}_0$ are set to zero on edges contained in the boundary $\partial\Omega$.

6.2. Importance Of Stabilization: EQS vs. SEQS. In order to demonstrate the robustness of the novel stabilized SEQS formulation (5.6) we use an example with an analytical solution of the EQS-equation (2.6). The configuration is shown in Figure 2. It consists of three conductive rectangular bars that are contained in a rectangular dielectric box. A voltage of $U_0 = 1\mathrm{V}$ (peak) is applied between the entire front- and back side of the box. On the other sides we use zero-flux boundary conditions. The material parameters are constant in each subdomain. They are chosen such that the ratio $\frac{\sigma}{\epsilon}$ is kept constant in x-direction, i.e. $\frac{\sigma^0}{\epsilon_r^o} = \frac{\sigma^i}{\epsilon_r^i}$. This yields

a spatially constant total current density in x direction

$$\mathbf{j}_{tot} = (\frac{\sigma}{\epsilon} + i\omega)\mathbf{D}, \text{ with } \mathbf{D} = D \cdot \mathbf{e}_x \text{ and } D = -U_0 \cdot \left(\frac{2 \cdot d^o}{\epsilon^o} + \frac{d^i}{\epsilon^i}\right)^{-1}.$$

Hence, the electric displacement field $\mathbf{D}$ is spatially constant and frequency-independent. In our example $D = -1.48 \cdot 10^{-10} \frac{\mathrm{C}}{\mathrm{m}^2}$ for the peak value. The electric field and the electric potential are also frequency-independent and can easily be calculated from $\mathbf{D}$.

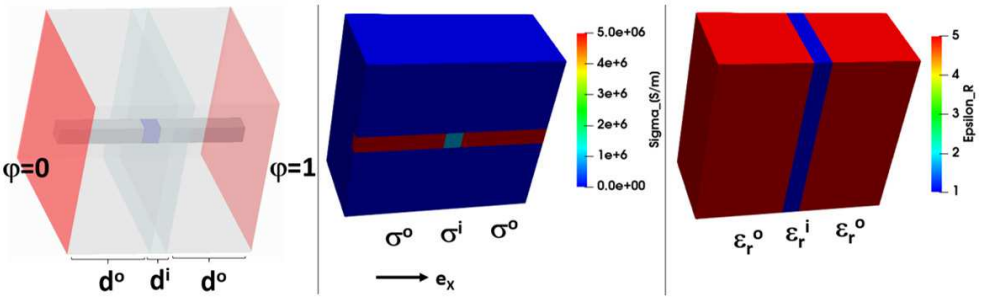

FIG. 2. *Conductive bars inside a dielectric box. The length of the sections are* $d^o = 10\,\mathrm{cm}$, $d^i = 2\,\mathrm{cm}$. *The entire front side of the box is grounded* ($V_1 = 0$) *and the entire back side is set to* $V_2 = 1$.

We solved the EQS problem (5.3) and the SEQS problem (5.6) by using a preconditioned BiCGstab method. The preconditioner for the EQS system was chosen based on the bilinear form

$$P_{EQS} \leftrightarrow \langle \sigma_l \, \mathbf{grad}(\widetilde{\varphi} + \Phi), \mathbf{grad}(\widetilde{\varphi}' + \Phi) \rangle_\Omega \ ,$$

with a lower bound for the coefficient $\sigma_l \leftarrow \max\{\sigma, \epsilon_r\}$ in order to guarantee regularity. The function Φ is the part of offset functions Φ_1 or Φ_2, for which the potential $V_{\mathrm{stat},1}$ or $V_{\mathrm{stat},2}$ is an unknown. The preconditioner for the SEQS system was chosen accordingly:

$$P_{SEQS} \leftrightarrow \begin{pmatrix} \langle \sigma_l \, \mathbf{grad}(\widehat{\varphi} + \Phi), \mathbf{grad}(\widehat{\varphi}' + \Phi) \rangle_\Omega & 0 \\ 0 & \langle \epsilon_r \, \mathbf{grad}\, \psi, \mathbf{grad}\, \psi' \rangle_{\Omega_A} \end{pmatrix}.$$

Both preconditioners are real-valued, symmetric, and positive definite. We stopped the iteration when the relative residual dropped below $1.0 \cdot 10^{-10}$. Throughout 4 iterations sufficed on a mesh with $\approx 400'000$ tetrahedral elements. Table 1 shows the resulting relative L^2 errors of the EQS/SEQS-solutions.

Frequency [Hz]	Rel. L^2-error $\mathbf{D}$ in Ω_A		Rel. L^2-error $\mathbf{D}$ in Ω_C	
	EQS	SEQS	EQS	SEQS
0	2.1	$9.2 \cdot 10^{-8}$	$9.2 \cdot 10^{-8}$	$9.2 \cdot 10^{-8}$
0.001	2.1	$9.2 \cdot 10^{-8}$	$9.2 \cdot 10^{-8}$	$9.2 \cdot 10^{-8}$
1	$4.4 \cdot 10^{-3}$	$9.2 \cdot 10^{-8}$	$9.2 \cdot 10^{-8}$	$9.2 \cdot 10^{-8}$
10	$5.1 \cdot 10^{-5}$	$9.2 \cdot 10^{-8}$	$9.2 \cdot 10^{-8}$	$9.2 \cdot 10^{-8}$
100	$7.6 \cdot 10^{-7}$	$9.2 \cdot 10^{-8}$	$9.2 \cdot 10^{-8}$	$9.2 \cdot 10^{-8}$
1000	$9.3 \cdot 10^{-8}$	$9.2 \cdot 10^{-8}$	$9.2 \cdot 10^{-8}$	$9.2 \cdot 10^{-8}$

TABLE 1

Relative errors of the electric displacement field in the dielectric and the conductive subdomain for the EQS and the SEQS solution at different frequencies. Owing to the extreme ill-conditioning of EQS for $\omega \approx 0$, some results are much affected by round-off errors.

The field is accurately calculated at any frequency in the conductive domain Ω_C with both EQS and SEQS. In the dielectric domain Ω_A, EQS at low frequencies incurs large errors, while the solution of the SEQS remains accurate, even at 0 Hz. Obviously, our stabilization works very well in this case.

6.3. Step II: Stabilized Maxwell. As a first example for the proposed two-step procedure we studied the correction to the electric field that resulted from the first step (SEQS) (5.6) by the second step (stabilized Maxwell) (5.12) for the case of the previous subsection 6.2. Figure 3 shows the results. At zero frequency the electric field is not corrected, because $\mathbf{E} = -\mathbf{grad}\,\varphi - i\omega\mathbf{A}$. So the plot on the left shows the constant SEQS solution. In the stationary case the second step is only required, if the magnetic field has to be calculated. The other two plots in Figure 3 show the total field, i.e. the SEQS solution $-\mathbf{grad}\,\varphi$ of the first step with the correction by $-i\omega\mathbf{A}$ of the second step. Note that in this specific case the SEQS solution is independent of the frequency! Thus the differences between the fields at 100 Hz/1000 Hz and the field at 0 Hz are in this figure exclusively due to the correction in the second step.

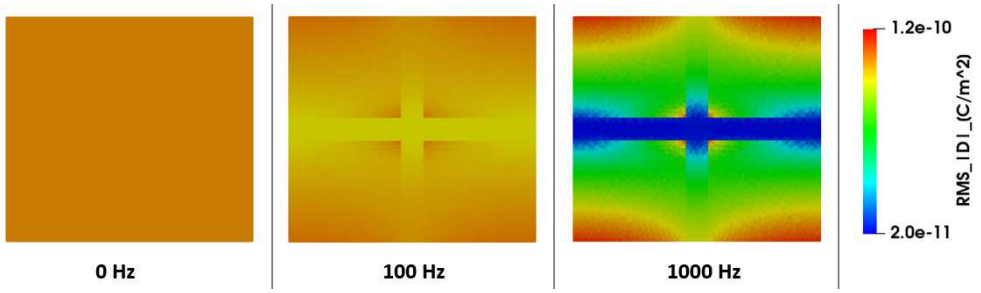

FIG. 3. *Electric displacement field (rms) at several frequencies.*

For testing purposes we also computed the field that resulted from first solving the SEQS system, and then solving the non-stabilized Maxwell system (5.9). As expected, we encountered stability problems at low frequencies $\omega > 0$ due to near-kernel fields in the non-conducting domain. These kind of problems are avoided, if the stabilized versions are used in both steps, as can be seen in Table 2: the correction of the SEQS field vanishes continuously for $\omega \to 0$, as required, if the stabilized Maxwell formulation is used to compute $\mathbf{A}$.

Frequency [Hz]	Rel. Difference **D** in Ω_A	Rel. Difference **D** in Ω_C
0	$9.2 \cdot 10^{-8}$	$9.2 \cdot 10^{-8}$
0.001	$9.6 \cdot 10^{-7}$	$4.6 \cdot 10^{-6}$
1	$9.5 \cdot 10^{-4}$	$4.6 \cdot 10^{-3}$
10	$9.5 \cdot 10^{-3}$	$4.6 \cdot 10^{-2}$
100	$8.6 \cdot 10^{-2}$	0.41
1000	0.2	0.97

TABLE 2

Relative L^2 differences of the electric displacement field between the analytical solution at 0 Hz and the solution of the combined SEQS / Stabilized Maxwell formulations (5.6)/(5.12) in the dielectric and the conductive subdomain at several frequencies.

For the solution of the stabilized Maxwell system we again used a preconditioned BiCGstab method with a real-valued, symmetric positive definite block-diagonal preconditioner $P_{SM} = \mathrm{diag}(M_A, M_f)$ with

$$M_A \leftrightarrow \left\langle \frac{1}{\mu}\,\mathbf{curl}\,\mathbf{A}_0, \mathbf{curl}\,\mathbf{A}_0' \right\rangle_\Omega + \left\langle \frac{\sigma_l\,\omega_l}{\mu_r}\,(\mathbf{A}_0 + \mathbf{grad}(\Phi_1+\Phi_2)), (\mathbf{A}_0' + \mathbf{grad}(\Phi_1+\Phi_2) \right\rangle_\Omega ,$$
$$M_f \leftrightarrow \langle \epsilon_r\,\mathbf{grad}(\nu + \eta_\mathbf{A}), \mathbf{grad}(\nu' + \eta_\mathbf{A}')\rangle_{\Omega_A} \ , \ \sigma_l \leftarrow \max\{\sigma, \epsilon_r\}\,, \ \omega_l \leftarrow \max\{\omega, 1\}\,.$$

We stopped the iteration when the relative residual became smaller than $1.0 \cdot 10^{-8}$, which never took more than 7 iterations.

6.4. An RLC Setup. We demonstrate the validity of our interpretation of the different terms of the field solution as static/induced voltages $U_{\mathrm{stat}}\,/\,U_{\mathrm{ind}}$, or as static/induced currents $I_{\mathrm{stat}}\,/\,I_{\mathrm{ind}}$, by comparison of these quantities with the analytical solution of a circuit model for the example of a RLC series circuit. The configuration that we use for this comparison is shown in Figure 4.

If a pure circuit model in frequency domain is used, then this configuration is described by Kirchhoff's voltage law for the voltages UR, UL, UC of the three circuit elements

$$U_{RLC} = \underbrace{R \cdot I_{RLC}}_{UR} + \underbrace{i\omega L \cdot I_{RLC}}_{UL} + \underbrace{\frac{1}{i\omega C} \cdot I_{RLC}}_{UC}\,, \tag{6.1}$$

with the periodic voltage source $U_{RLC} = U_0 \cdot e^{i\omega t}$, and the total current I_{RLC} (or I_{RC} in case of vanishing inductance L).

6.4.1. Imposed Voltage. We first fixed the exterior resistance to $R_{ext} = 450\,\mathrm{m}\Omega$ and calculated the field and the circuit solutions in the case of a voltage source of $U = 1\,\mathrm{V}\,(rms)$. Figure 5 shows the resulting currents. The dotted black line is the current I_{RC} of a RC-circuit that neglects the inductance. The (quasi)static current I_{stat} that was computed by solving the SEQS system (5.6) is marked with blue points. We observe an excellent match.

The black solid line represents the current I_{RLC} of a RLC-circuit. We get the total current $I = I_{\mathrm{stat}} + I_{\mathrm{ind}}$ (marked with red dots) by adding to it the induced current I_{ind} obtained by solving the stabilized Maxwell system (5.12). It also agrees very well with the RLC-circuit model; only the peak value at resonance is slightly lower.

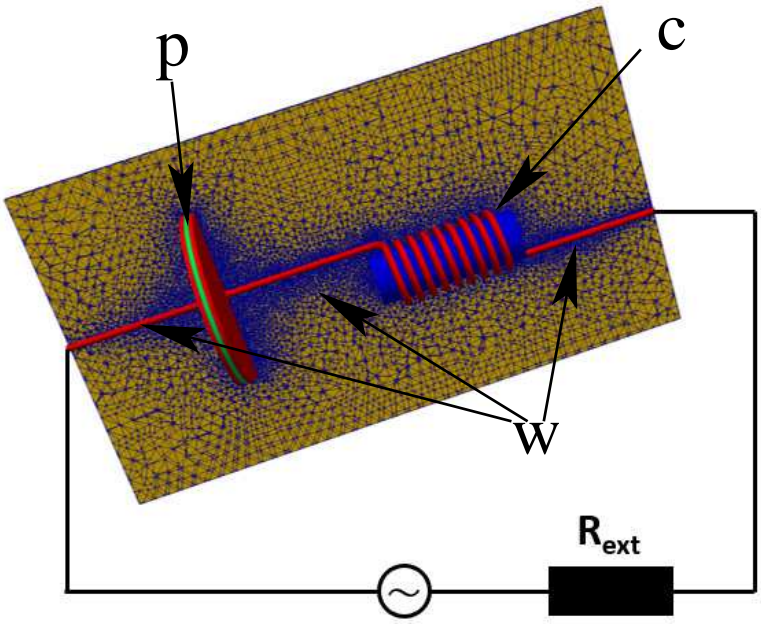

FIG. 4. *RLC Series circuit. The capacitor and the inductance in the field domain is coupled to a resistor and a voltage or current AC source in the circuit domain. The plate capacitor has a radius of* 6 cm*, the plate distance is* 3 *mm, the relative permittivity of the dielectric between the plates is* $\epsilon_r = 1.0 \cdot 10^6$*, which yields an approximate capacity of* $C = 33.4\,\mu\mathrm{F}$*. The coil with 8 windings has a length of* 9 cm*, the inner radius is* 17 mm*, and the magnetic core has a relative permeability of* $\mu_r = 1000$*. This yields an inductance of* $L = 10.1\,\mu\mathrm{H}$*, which we calculated with a field solver at* 50 Hz*. The wire with electrical conductivity of* $\sigma = 1.0 \cdot 10^7\,\mathrm{S/m}$ *has a diameter of* 5 mm*, and the total resistance of the configuration in the field domain was computed to* $R_L = 7.2\,\mathrm{m\Omega}$*. The resonance frequency in our example of a RLC series circuit is at* 8671 Hz*.*

The phase shift between the applied voltage and the resulting current are shown in Figure 6 for the circuit model and the field model. There is again a perfect match between the phase shift of the SEQS field solution and the phase shift of the RC-circuit. After correction of this phase shift by the stabilized Maxwell model there is agreement with the phase shift according to the RLC-circuit.

6.4.2. Imposed Current. In the next example we compared the different contributions of the total voltage that were calculated by the field model with the voltages of the circuit model. We therefore set the external resistance R_{ext} to zero and imposed a current of $I = 1\,\mathrm{A}\,(rms)$. In the field model the resulting total voltage $U = U_{\mathrm{stat}} + U_{\mathrm{ind}}$ consists of the static voltage U_{stat} that results from the SEQS solution of (5.6), and the induced voltage U_{ind} of the Maxwell correction (5.12). Similarly as in the previous section there is agreement between the static voltage U_{stat}, and the voltages UR, UC of the RC-circuit. The imaginary part of the inductive voltage U_{ind} corresponds to the voltage UL that drops at the inductance in case of the RLC-circuit. The only yet unclear contribution is the real part of the induced voltage. It is small compared to the other components, e.g. at resonance it is 0.024 V. This voltage originates from the increase of the resistance due to the skin effect, and explains the reduced peak current at resonance in Figure 5.

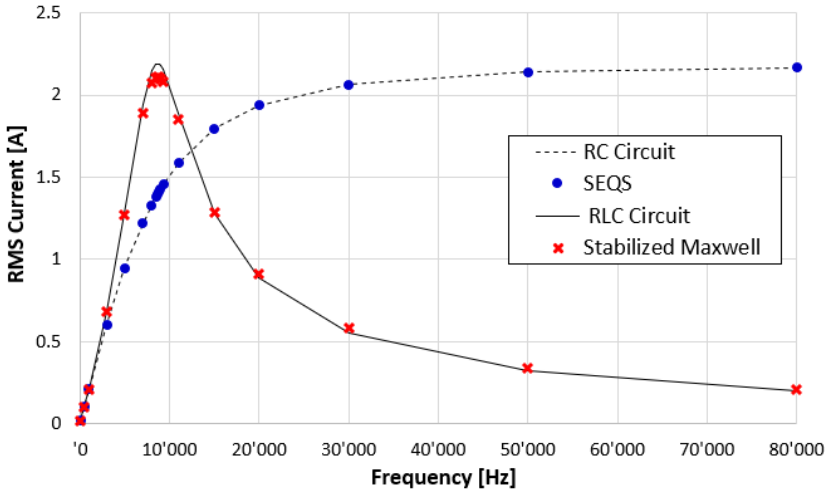

FIG. 5. *Comparison of the current - FEM model vs circuit model.*

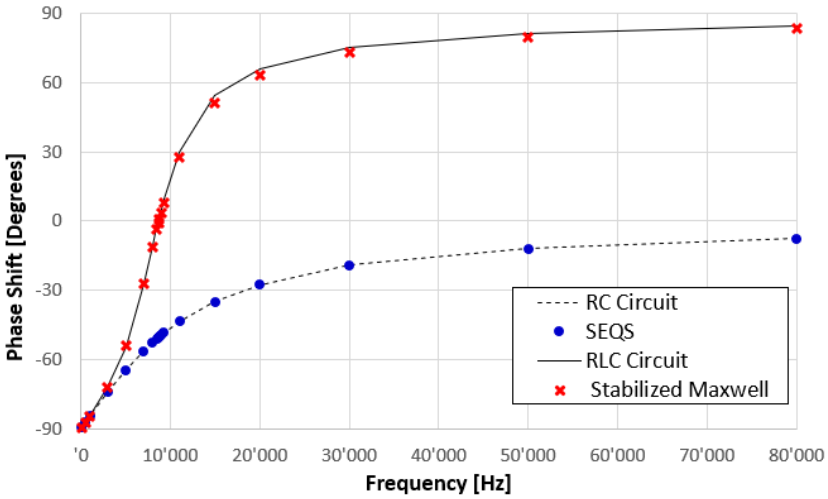

FIG. 6. *Comparison of the phase shift - FEM model vs circuit model.*

6.4.3. Voltage Source. In our final numerical experiment we studied the different contributions to the electric field $\mathbf{E} = -\mathbf{grad}\,\varphi - i\omega\mathbf{A}$ at different frequencies. We switched back to a voltage source with $U = 1\,\mathrm{V}\,(rms)$ and removed the external resistor. The results are shown in Figure 8. The field is dominated by the contribution of the electric scalar potential at low frequencies, and at higher frequencies it is necessary to include inductive effects, as expected.

For the field solution we used the same tetrahedral mesh for all calculations of the RLC-circuit of subsection 6.4. It consists of 1.12 million elements. We used the preconditioned iterative solvers as described in subsection 6.2, and in subsection 6.3. The iterations in Step I were stopped after a relative residual of $1.0{\cdot}10^{-10}$ was reached, which never took more than 6 iterations. We stopped the iterations in Step II after a relative residual of $1.0 \cdot 10^{-8}$ was reached, which took at most 30 iterations.

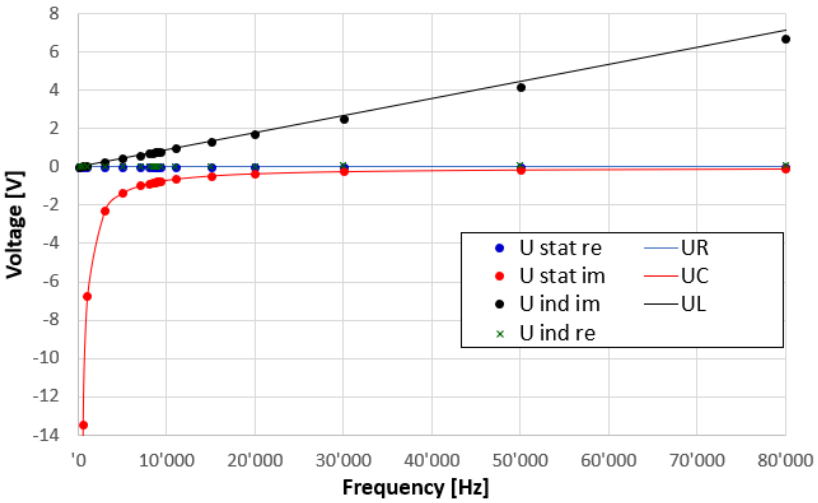

FIG. 7. *Comparison of the voltage - FEM model vs circuit model.*

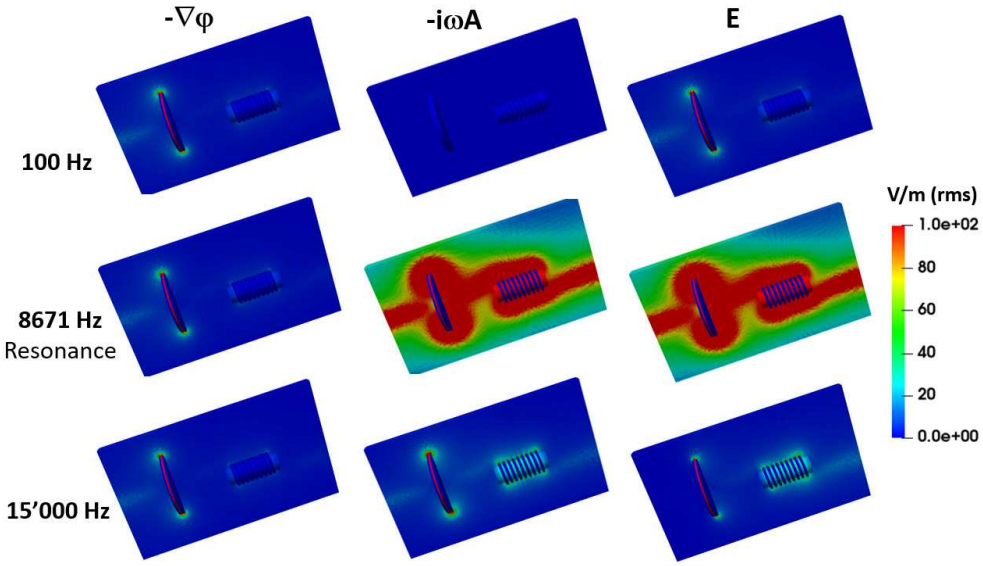

FIG. 8. *Comparison of the different contributions to the E-field.*

7. Conclusion. In this article we showed that capacitive/resistive and magnetic/inductive effects can consistently be calculated in two *sequential* steps. We introduced an efficient, *frequency stable* finite-element discretization and demonstrated how the fields obtained in the two steps can be interpreted. The main ideas can be extended beyond a finite-element framework.

REFERENCES

[1] A. ALONSO-RODRIGUEZ AND A. VALLI, *Eddy Current Approximation of Maxwell Equations*,

vol. 4 of Modelling, Simulation & Applications, Springer, Milan, 2010.

[2] Z. Badics and J. Pávó, *Full wave potential formulation with low-frequency stability including Ohmic losses*, IEEE Transactions on Magnetics, 51 (2015), pp. 1–4, https://doi.org/10.1109/TMAG.2014.2362114.

[3] G. Ciuprina, D. Ioan, R. Janssen, and E. van der Heijden, *MEEC models for RFIC design based on coupled electric and magnetic circuits*, IEEE Transactions on Computer-Aided Design of Integrated Circuits and Systems, 34 (2015), pp. 395–408, https://doi.org/10.1109/TCAD.2014.2387863.

[4] G. Ciuprina, D. Ioan, M. Popescu, and S. Lup, *Electric Circuit Element Boundary Conditions in the Finite Element Method for Full-Wave Frequency Domain Passive Devices*, Submitted to Scientific Computing in Electrical Engineering, Eindhoven, Springer, 2020.

[5] M. Eller, S. Reitzinger, S. Schöps, and S. Zaglmayr, *A symmetric low-frequency stable broadband Maxwell formulation for industrial applications*, SIAM Journal on Scientific Computing, 39 (2017), pp. B703–B731.

[6] H. Haus and J. Melcher, *Electromagnetism, Chapter 3: Limits to statics and quasistatics*, MIT Open Course, (2016), http://web.mit.edu/6.013_book/www/book.html.

[7] R. Hiptmair, F. Krämer, and J. Ostrowski, *A robust Maxwell formulation for all frequencies*, IEEE Transactions on magnetics, 44 (2008), pp. 682–685.

[8] R. Hiptmair and J. Ostrowski, *Electromagnetic port boundary conditions: Topological and variational perspective*, International Journal of Numerical Modelling: Electronic Networks, Devices and Fields, n/a (2021), p. e2839, https://doi.org/https://doi.org/10.1002/jnm.2839, https://onlinelibrary.wiley.com/doi/abs/10.1002/jnm.2839, https://arxiv.org/abs/https://onlinelibrary.wiley.com/doi/pdf/10.1002/jnm.2839.

[9] S. L. Ho, Y. Zhao, W. N. Fu, and P. Zhou, *Application of edge elements to 3-d electromagnetic field analysis accounting for both inductive and capacitive effects*, IEEE Transactions on Magnetics, 52 (2016), pp. 1–4, https://doi.org/10.1109/TMAG.2015.2483620.

[10] D. Ioan, W. Schilders, G. Ciuprina, N. v. d. Meijs, and W. Schoenmaker, *Models for integrated components coupled with their EM environment*, COMPEL: Int J for Computation and Maths. in Electrical and Electronic Eng., 27 (2008), pp. 820–829.

[11] M. Jochum, O. Farle, and R. Dyczij-Edlinger, *A new low-frequency stable potential formulation for the finite-element simulation of electromagnetic fields*, IEEE Transactions on Magnetics, 51 (2015), pp. 1–4, https://doi.org/10.1109/TMAG.2014.2360080.

[12] S. Koch, H. Schneider, and T. Weiland, *A low-frequency approximation to the Maxwell equations simultaneously considering inductive and capacitive phenomena*, IEEE Transactions on Magnetics, 48 (2012), pp. 511–514, https://doi.org/10.1109/TMAG.2011.2173163.

[13] T. Steinmetz, S. Kurz, and M. Clemens, *Domains of validity of quasistatic and quasistationary field approximations*, in VXV International Symposium on Theoretical Engineering, June 2009, pp. 1–5.

[14] Y. Zhao and W. N. Fu, *A new stable full-wave Maxwell solver for all frequencies*, IEEE Transactions on Magnetics, 53 (2017), pp. 1–4, https://doi.org/10.1109/TMAG.2016.2646372.

[15] Y. Zhao and Z. Tang, *A novel gauged potential formulation for 3-d electromagnetic field analysis including both inductive and capacitive effects*, IEEE Transactions on Magnetics, 55 (2019), pp. 1–5, https://doi.org/10.1109/TMAG.2019.2899288.

[16] Y. Zhao and Z. Tang, *A symmetric field-circuit coupled formulation for 3-d transient full-wave maxwell problems*, IEEE Transactions on Magnetics, 55 (2019), pp. 1–4, https://doi.org/10.1109/TMAG.2019.2896647.